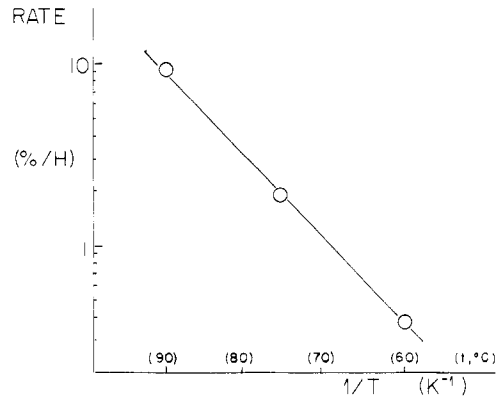

Figure 3. log of the initial reaction rate vs. reciprocal temperature. The solid line represents an Arrhenius law with an activation energy of 19 kcal/mol. H ≡ hour.

sample at 75 °C for 19 h, during which time we monitored the monomer concentration, as shown typically in Figures 1 and 2. After stopping the reaction, we determined the polymer conversion classically by first dissolving the polymerized sample in 1,4-dioxane and then precipitating the polystyrene in methyl alcohol.[8] We found an 18% conversion by the classical method and a 21% conversion based on Raman scattering. The agreement is quite reasonable, especially in view of the fact that there must be a residual amount of oligomers which are not precipitated by the classical method.

Conclusion

We have presented a new method for studying polymerization reactions based on Raman scattering. This method is fairly general, easy to use and to automate, and insensitive to most spurious phenomena. We have illustrated this method by a study of the thermal polymerization of styrene at different temperatures and found our results to be in essential agreement with those obtained by other methods.

Acknowledgment. We gratefully acknowledge support from the U.S. Army Research Office. G.Z. gratefully acknowledges support from Conseiller Culturel de l'Ambassade de France and the Service de l'Enseignement et des Echanges Linguistiques—Ministère des Affaires Etrangères (Paris). We thank Day-Chyuan Lee for his help in performing the Raman studies and the chemical analysis on the polystyrene content and Kirk J. Abbey for a helpful discussion.

References and Notes

(1) Patterson, G. D.; Stevens, J. R.; Alms, G. R.; Lindsey, C. P. *Macromolecules* **1979**, *12*, 658.
(2) Patterson, G. D.; Stevens, J. R.; Alms, G. R.; Lindsey, C. P. *Macromolecules* **1979**, *12*, 661.
(3) Coakley, R. W.; Mitchell, R. S.; Hunt, J. L.; Stevens, J. R. *J. Macromol. Sci., Phys.* **1976**, *12*, 511.
(4) Alms, G. R.; Patterson, G. D.; Stevens, J. R. *J. Chem. Phys.* **1979**, *70*, 2145.
(5) Jeffrey, K. R.; Stevens, J. R. *J. Chem. Phys.* **1979**, *71*, 2331.
(6) O'Driscoll, K. F.; Wertz, W.; Husar, A. *J. Polym. Sci., Part A-1* **1967**, *5*, 2159.
(7) Cardenas, J. N.; O'Driscoll, K. F. *J. Polym. Sci., Polym. Chem. Ed.* **1977**, *15*, 1883.
(8) See, e.g.: Boundy, R. H.; Boyer, R. F., Eds. "Styrene, Its Polymers, Copolymers and Derivatives"; Hofner Publishing Company: New York, 1952.

Phase Behavior of Reversibly Polymerizing Systems with Narrow Length Distributions

Judith Herzfeld*
Biophysical Laboratory, Harvard Medical School, Boston, Massachusetts 02115
Robin W. Briehl
Departments of Biochemistry and Physiology, Albert Einstein College of Medicine, Bronx, New York 10461. *Received May 23, 1980*

ABSTRACT: The lattice models of Flory and DiMarzio for rigid linear polymers of fixed length have been extended to describe reversibly polymerizing systems with narrowly distributed polymer lengths (i.e., it is assumed that the system remains approximately monodisperse as the average polymer length varies with concentration and other variables). Whereas irreversibly polymerized systems are expected to form a relatively dilute, partially aligned anisotropic phase unless sufficiently strong attractions between polymers are present to condense them, we find that reversibly polymerizing systems are expected to form a highly concentrated and highly ordered anisotropic phase unless sufficiently strong repulsions between polymers are present to separate them. The predicted temperature dependence of the phase behavior for the two systems is markedly different. For the reversibly polymerizing system there exists a temperature below which there is no phase transition at any concentration of solute. Just above this temperature there is a wide two-phase region in which a dilute isotropic phase, consisting of monomers or very short polymers, is in equilibrium with a quasi-crystalline phase consisting of very long, highly aligned polymers which essentially completely exclude solvent. The decrease in the concentration of the isotropic phase, with increasing temperature, occurs at a progressively decreasing rate to give an "elbow-shaped" phase boundary. The anisotropic phase remains very dense at high temperatures unless the interactions between polymers are sufficiently repulsive to separate them and admit solvent. The temperature dependence of the viscosity of sickle-cell hemoglobin solutions is consistent with the theoretical predictions. Interpretation of the experimental data in terms of the model suggests that domain dimensions could be a major determinant of the viscous properties of these sickle-cell hemoglobin solutions and could account for some of the hysteresis observed in these systems.

Introduction

If the axial ratio is large enough and the concentration high enough, long rodlike particles will align spontaneously, even in the absence of intermolecular interactions, as a consequence of excluded volumes. The theory for phase transitions of this type has been developed by Onsager,[1] Isihara,[2] and Zwanzig[3] for dilute solutions, using a virial expansion, and by Flory[4] and DiMarzio[5] for the full range

0024-9297/81/2214-0397$01.25/0

of concentrations, using lattice models. The main predictions of the theory have been confirmed by experiments on α-helical polypeptides[6-11] and p-phenylene polyamides.[12-15]

The above theories assume that all the polymers in the system are of the same length (monodispersity) and that the polymer length is fixed (irreversible polymerization). In this case, moderately long noninteracting rods will separate into two phases only in a narrow range of concentrations, the isotropic phase being only slightly less concentrated than the anisotropic phase. As rod length increases, the two-phase region gradually narrows and moves to lower concentrations (the concentrations of the coexisting isotropic and anisotropic phases both decreasing).

From these results one can anticipate how more complicated systems will behave. In a polydisperse system, the larger rods would be expected to partition preferentially into the anisotropic phase while the shorter rods partition preferentially into the isotropic phase, thus creating the potential for the coexistence of more than two phases. Flory et al. have recently shown that this is indeed the case.[16-19]

In a reversibly polymerizing system, rod length can change with concentration to minimize the free energy. Since increasing rod length favors alignment, it is to be expected that alignment will also favor polymerization and that this reciprocal coupling of orientation and polymerization will result, even in the absence of interparticle interactions, in a very wide two-phase region in which a very dilute isotropic phase consisting of relatively short molecules coexists with a very concentrated and very highly ordered anisotropic phase consisting of very long molecules. We have previously reported[20] that this expectation is confirmed by calculations based on an extension of Flory's lattice model. Here we present the details of those calculations and also demonstrate that essentially the same conclusions may be drawn from an extension of DiMarzio's lattice model. The phase diagrams obtained are radically different from those for fixed-length rods and are discussed in relation to the phase behavior of sickle-cell hemoglobin.

Extension of Flory's Lattice Model

Flory has computed the statistics for arranging a monodisperse collection of rods of length x on a lattice, at an angle ψ relative to the axis of alignment, by dividing the rods into $y = x \sin \psi$ equal lengths lying on adjacent rows of the lattice (see Figure 1 of ref 4). According to this model, the free energy ΔG_m of mixing n_2 rods of length x with n_1 solvent molecules depends on y according to the expression

$$\Delta G_m/RT = n_1 \ln v_1 + n_2 \ln v_2 - (n_1 + yn_2) \ln [1 - v_2(1 - y/x)] - n_2[\ln (xy^2) - y + 1] + xn_2v_1\chi \quad (1)$$

where $v_1 = n_1/(n_1 + xn_2)$ and $v_2 = xn_2/(n_1 + xn_2)$ are the volume fractions of solvent and solute, respectively, and $RT\chi$ is the free energy of interaction between rods, which is assumed to be small enough that rod positions for a specific orientation remain random. The system of fixed-length rods equilibrates at the value of y which minimizes ΔG_m.

If the rods are formed by reversible polymerization, then polymer lengths, as well as orientations, will adjust to the value which minimizes the free energy. If the resulting length distribution is narrow, the orientation contribution to the free energy may be approximated by ΔG_m in eq 1. In addition, the free energy of polymerization must be taken into account. For simple linear polymerization of quasi-spherical particles, a polymer of length x has $(x - 1)$ identical linkages. The free energy of polymerization is then given by

$$\Delta G_p/RT = (x - 1)n_2\phi \quad (2)$$

where ϕRT is the free energy of formation of a single linkage. The complete free energy, ΔG, is thus given by the sum

$$\Delta G = \Delta G_m + \Delta G_p \quad (3)$$

and the system equilibrates at the values of single and y which minimize ΔG.

Since n_2 varies inversely with x, it is convenient to divide eq 3 by $(n_1 + xn_2)$ to give the free energy per unit volume

$$f = v_1 \ln v_1 + \frac{v_2}{x} \ln v_2 - \left(v_1 + \frac{y}{x}v_2\right) \ln \left(v_1 + \frac{y}{x}v_2\right) - \frac{v_2}{x}[\ln (xy^2) - y + 1] + v_1v_2\chi + \frac{x - 1}{x}v_2\phi \quad (4)$$

We then locate the minimum of f, for a system of a given composition, v_1, and v_2 in the region $1 \leq y \leq x$. Local minima occur at those points where $\partial f/\partial y = 0$, $\partial f/\partial x = 0$, $\partial^2 f/\partial y^2 > 0$, $\partial^2 f/\partial x^2 > 0$ and $\Delta = (\partial^2 f/\partial y^2)(\partial^2 f/\partial x^2) - (\partial^2 f/\partial x \partial y)^2 > 0$. Differentiation of eq 4 gives

$$\frac{\partial f}{\partial y} = -\frac{v_2}{x}\left[\ln \left(v_1 + \frac{y}{x}v_2\right) + \frac{2}{y}\right] \quad (5a)$$

$$\frac{\partial f}{\partial x} = -\frac{v_2}{x}\left[\ln v_2 - \ln (xy^2) - y \ln \left(v_1 + \frac{y}{x}v_2\right) - \phi\right] \quad (5b)$$

and

$$\frac{\partial^2 f}{\partial y^2} = -\frac{v_2}{x}\left(\frac{v_2/x}{v_1 + yv_2/x} - \frac{2}{y^2}\right) \quad (6a)$$

$$\frac{\partial^2 f}{\partial x \partial y} = -\frac{1}{x}\frac{\partial f}{\partial y} + \frac{yv_2^2/x^3}{v_1 + (y/x)v_2} \quad (6b)$$

$$\frac{\partial^2 f}{\partial x^2} = -\frac{1}{x}\frac{\partial f}{\partial x} + \frac{v_2}{x^3}\left(1 - \frac{y^2v_2/x}{v_1 + yv_2/x}\right) \quad (6c)$$

In the Appendix we show that the two first derivatives are zero at either two points in the region $0 < y < x$ or at no points at all and that, of the possible two points, only one corresponds to a local minimum in f.

The absolute minimum of f is determined by comparing the value of f at the above local minimum, if it occurs in the region $1 \leq y$, with the minimum values of f attained on the boundaries $y = 1$ and $y = x$. For $y = 1$, the perfectly ordered limit

$$\frac{\partial f}{\partial x} = -\frac{v_2}{x}\left[\ln v_2 - \ln x - \ln \left(v_1 + \frac{1}{x}v_2\right) - \phi\right] \quad (7a)$$

$$\frac{\partial^2 f}{\partial x^2} = -\frac{1}{x}\frac{\partial f}{\partial x} + \frac{v_1v_2}{x^2(v_1 + v_2/x)} \quad (7b)$$

and an extremum occurs for

$$x = \frac{v_2}{v_1}(e^{-\phi} - 1) \quad (7c)$$

which is a minimum when $\phi < 0$ and a maximum when $\phi > 0$. For $y = x$, the isotropic limit,

$$f = v_1 \ln v_1 + \frac{v_2}{x} \ln v_2 - \frac{v_2}{x}(3 \ln x - y + 1) + v_1 v_2 \chi + \frac{x-1}{x} v_2 \phi \quad (8a)$$

$$\frac{\partial f}{\partial x} = \frac{v_2}{x^2}(-\ln v_2 + 3 \ln x - 2 + \phi) \quad (8b)$$

$$\frac{\partial^2 f}{\partial x^2} = -\frac{2}{x}\frac{\partial f}{\partial x} + \frac{3v_2}{x^3} \quad (8c)$$

and a minimum in f occurs at

$$x^3 = v_2 e^{2-\phi} \quad (8d)$$

For a system of a given composition v_1 and v_2, the values of x and y corresponding to the absolute minimum in f describe the equilibrium state of the system, from which the chemical potentials of the solvent and solute can be determined by the relationships

$$\frac{\mu_1}{RT} = \frac{\partial(\Delta G/RT)}{\partial m_1} = f + v_2\left(\frac{\partial f}{\partial v_1} - \frac{\partial f}{\partial v_2}\right) \quad (9a)$$

and

$$\frac{\mu_2}{RT} = \frac{\partial(\Delta G/RT)}{\partial m_2} = f + v_1\left(\frac{\partial f}{\partial v_2} - \frac{\partial f}{\partial v_1}\right) \quad (9b)$$

where $m_1 = n_1$ and $m_2 = xn_2$ are the total amounts of solvent and solute present. From these chemical potentials, phase diagram can be constructed analogous to the phase diagrams for irreversibly polymerized molecules (see Figures 1 and 2 of ref 20).

Extension of DiMarzio's Lattice Model

DiMarzio's lattice model[5] is a simplification of Flory's model in that the continuum of rod orientations allowed in Flory's model is replaced by a finite discrete set of allowed orientations in DiMarzio's model. In particular we have chosen the simplest case in which the rods are permitted to lie only in the directions of the three mutually orthogonal axes of the simple cubic lattice. Due to this restriction of paarticle orientations, the model samples narrow orientation distributions less well than Flory's model.[21] On the other hand, violation of spherical symmetry in the latter model[22] (reflected in Figure 1 of ref 4 in the fact that the projection of a rod of length x on the axis of alignment is equal to x for all values of ψ) causes it to break down for orientations at large angles relative to the preferred direction.[23] The importance of these differing limitations, in the present context, may be assessed by employing both approaches and comparing the results.

Free Energy Function. DiMarzio[5] has shown that the number of ways of arranging N_i, N_j, and N_k rods of length x in the directions of the i, j, and k axes, respectively, of a lattice of N cells is

$$g(x,N_i,N_j,N_k,N) = \frac{(N-(x-1)N_i)!(N-(x-1)N_j)!(N-(x-1)N_k)!}{N!^2 N_i! N_j! N_k! (N-x(N_i+N_j+N_k))!} \quad (10)$$

The total solute in this system is $m_2 = x(N_i + N_j + N_k)$ and the total solvent is $m_1 = N - x(N_i + N_j + N_k)$. For an isotropic system, all lattice axes are equivalent and $N_i = N_j = N_k$. If we make the reasonable assumption that, even in an anisotropic system, two of the lattice axes will be equivalent, i.e., $N_j = N_k$, then it is possible to define an orientation parameter $y = N_i/(N_i + N_j + N_k)$, which varies from 1 for perfect axial alignment, to 1/3 for an isotropic distribution, to 0 for a planar array. In this notation, the degeneracy factor may be rewritten as

$$g(z,y,m_1,m_2) = \frac{[(m_1+m_2) - zym_2]!\left[(m_1+m_2) - z\left(\frac{1-y}{2}\right)m_2\right]!^2}{(m_1+m_2)!\left[\left(\frac{1-y}{2}\right)(1-z)m_2\right]!^2[y(1-z)m_2]!m_1!} \quad (11)$$

where $z = (x-1)/x$ is a convenient rod length parameter, varying from 0, for monomers, to 1, for rods of infinite length.

Minton has adopted a square-well potential for interactions between rods and used a Bragg–Williams-type approximation to derive an expression for the free energy of interactions of the form

$$U(z,y,m_1,m_2)/RT = w_{\parallel} N_{\parallel} + w_{\perp} N_{\perp} \quad (12)$$

where $N_{\parallel}$ and $N_{\perp}$ are the numbers of parallel and perpendicular contacts between rods, respectively.[24] For sufficiently small values of $w_{\parallel}$ and $w_{\perp}$, the distribution of rods in each diirection may be assumed to be random and

$$N_{\parallel} = \frac{x^2}{2N}(N_i^2 + N_j^2 + N_k^2) = \frac{m_2^2}{m_1+m_2}(1 - 2y + 3y^2)/4 \quad (13a)$$

$$N_{\perp} = \frac{x^2}{2N}(2N_iN_j + 2N_jN_k + 2N_kN_i) = \frac{m_2^2}{m_1+m_2}(1-y)(1+3y)/4 \quad (13b)$$

so that

$$\frac{U(z,y,m_1,m_2)}{RT} = \frac{m_2^2}{m_1+m_2}\left[\delta\left(\frac{1}{2} - y + \frac{3}{2}y^2\right) + w_{\perp}\right]\Big/ 2 \quad (14)$$

where $\delta = w_{\parallel} - w_{\perp}$.

For a reversibly polymerizing system, the free energy of polymerization must be included (from eq 2) and the complete expression for the free energy is

$$\frac{\Delta G}{RT} = -\ln g(z,y,m_1,m_2) + \frac{U(z,y,m_1,m_2)}{RT} + zm_2\phi \quad (15)$$

Using Stirling's approximation, $\ln N! \cong N \ln N - N$

$$f = \frac{1}{m_1+m_2}\frac{\Delta G}{RT} = v_1 \ln v_1 - g_1 \ln g_1 - 2g_2 \ln g_2 + g_3 \ln g_3 + 2g_4 \ln g_4 + v_2^2\left[\delta\left(\frac{1}{2} - y + \frac{3}{2}y^2\right) + w_{\perp}\right]\Big/ 2 + zv_2\phi \quad (16)$$

where

$$g_1 = 1 - zyv_2 \quad (17a)$$

$$g_2 = 1 - z(1-y)v_2/2 \quad (17b)$$

$$g_3 = y(1-z)v_2 \quad (17c)$$

$$g_4 = (1-y)(1-z)v_2/2 \quad (17d)$$

and

$$\frac{\partial f}{\partial z} = v_2\left(y \ln \frac{g_1}{g_3} + (1-y) \ln \frac{g_2}{g_4} + \phi\right) \quad (18a)$$

$$\frac{\partial f}{\partial y} = v_2\left[z \ln \frac{g_1}{g_2} + (1-z) \ln \frac{g_3}{g_4} + v_2\frac{\delta}{2}(3y-1)\right] \quad (18b)$$

$$\frac{\partial^2 f}{\partial z^2} = \frac{v_2}{(1-z)}\left[\frac{y(1-yv_2)}{g_1} + \frac{(1-y)(1-(1-y)v_2/2)}{g_2}\right] \quad (18c)$$

$$\frac{\partial^2 f}{\partial y \partial z} = v_2\left[\ln\frac{(1-y)g_1}{2yg_2} - \frac{zv_2(3y-1)}{2g_1g_2}\right] \quad (18d)$$

$$\frac{\partial^2 f}{\partial y^2} = v_2\left[\frac{1-z}{y(1-y)} - \frac{v_2z^2(3-zv_2)}{2g_1g_2} + \frac{3}{2}\delta v_2\right] \quad (18e)$$

The loci of points in the region $0 \le y \le 1$ and $0 \le z \le 1$ for which $\partial f/\partial z = 0$ and for which $\partial f/\partial y = 0$ are shown in Figure 1. The value of z for which $(\partial f/\partial z)_{y=1/3} = 0$ is

$$\tilde{z} = (e^{-\phi} - 3/v_2)/(e^{-\phi} - 1) \quad (19)$$

$0 < \tilde{z} < 1$ if $\phi < \ln(v_2/3)$ and $\tilde{z} < 0$ if $\ln(v_2/3) < \phi < 0$. The value of z for which $(\partial^2 f/\partial y^2)_{y=1/3} = 0$ is

$$\hat{z} = (9 + 3\delta v_2)/(9 + 3v_2 + \delta v_2^2) \quad (20)$$

For those values of δ for which eq 13 is valid (i.e., $|\delta|$ small), $0 < \hat{z} < 1$.

Figure 1 shows the various minima which we locate numerically. When more than one local minimum is obtained, f is evaluated for each to determine which is the absolute minimum. Figure 2, parts a and b, shows the dependence of the equilibrium values of $x = (1-z)^{-1}$ and y on the composition of the system, v_2, for $\delta = 0$ and various values of ϕ. An abrupt increase in both variables occurs at the phase transition. In contrast, the alignment transition for irreversibly polymerized molecules occurs with a more gradual change in y (Figure 2c).

Phase Behavior. Using the equilibrium values of z and y, one may calculate the chemical potentials of solute and solvent by combining eq 9, 16, and 17. The resulting phase boundaries are illustrated in Figure 3a. These phase diagrams show essentially the same features as those in Figure 2 of ref 20, obtained by using Flory's lattice model. As for irreversibly polymerized systems (Figure 3b here and Figure 1 in ref 20), all the phase diagrams are stemlike. However, when polymerization is irreversible, the stem in the phase diagram extends into the region of attractive interactions (positive values of χ, negative values of $w_\parallel$ and $w_\perp$); when polymerization is reversible the stem ends in the region of repulsive interactions. Thus, in the athermal case (χ, $w_\parallel$, $w_\perp = 0$), phase separation occurs over a very wide range of concentrations in the reversibly polymerizing system but only over a narrow range of concentrations in the irreversibly polymerized system. For the reversibly polymerizing system, the anisotropic phase essentially completely excludes solvent, unless sufficiently repulsive forces are acting between polymers to cause them to be less closely packed. For irreversibly polymerized molecules, on the other hand, the anisotropic phase is relatively dilute unless sufficiently attractive forces are acting between polymers to induce a miscibility transition which merges with the alignment transition. Even then (i.e., below the stem), $v_2 < 1$ for the anisotropic phase in the irreversibly polymerized system, whereas $v_2 \to 1$ for the anisotropic phase in the reversibly polymerized system. For the irreversibly polymerized system with sufficiently long rods, there is a narrow region, at the bottom of the stem, in which the miscibility transition is distinct from the alignment transition and two anisotropic phases may coexist; such a region does not occur for the reversibly polymerizing system. If the polymer length is decreased in the irrversibly polymerized system, the stem broadens and moves to higher values of v_2, and the base of the stem moves further into the region of attractive interactions. If the free energy of polymerization is increased in the reversibly polymerized system, the stem also broadens and moves to higher values of v_2, but the base of the stem moves further into the region of repulsive interactions. The two systems most closely approximate one another when the irreversibly polymerized molecules are very long and the free energy of reversible polymerization is very negative.

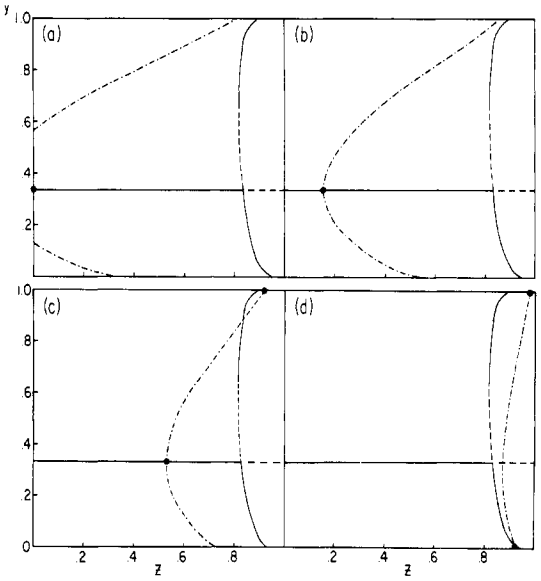

Figure 1. Loci of points in the y,z plane for which $\partial f/\partial z = 0$ (-·-), loci of points in the y,z plane for which $\partial f/\partial y = 0$ and $\partial^2 f/\partial y^2 > 0$ (—) or $\partial^2 f/\partial y^2 < 0$ (---), and minima of the free energy function (●) for $v_2 = 0.6$, $\delta = 0.00$, and (a) $\phi = -1.5$, (b) $\phi = -1.75$, (c) $\phi = -2.25$, and (d) $\phi = -3.5$. In the right-hand side of the plane $\partial f/\partial z > 0$ and in the left-hand side $\partial f/\partial z < 0$. In the upper right and lower left corners of the plane $\partial f/\partial y < 0$ and in the upper left and lower right corners $\partial f/\partial y > 0$.

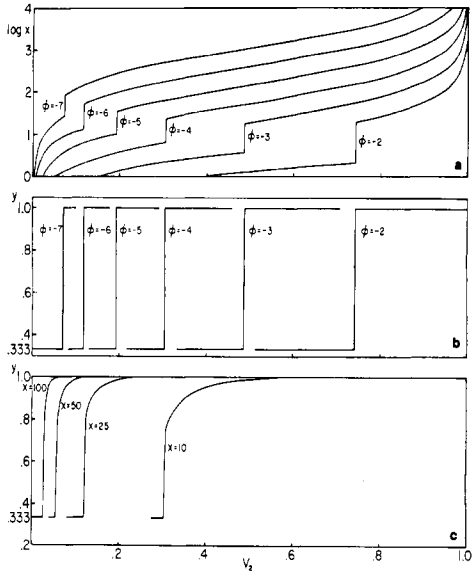

Figure 2. (a,b) Dependence of x and y on v_2 for reversible polymerization with $\delta = 0.000$ and various values of ϕ as indicated. (c) Dependence of y on v_2 for irreversible polymerization with $\delta = 0.000$ and various values of x as indicated.

Polymer lengths in the coexisting phases are indicated in Figure 4 by the symbols demarcating the boundaries of the two-phase region. We find that, in the absence of interpolymer interactions ($w_\parallel = w_\perp = 0$), phase separation coincides with the onset of polymer formation and that,

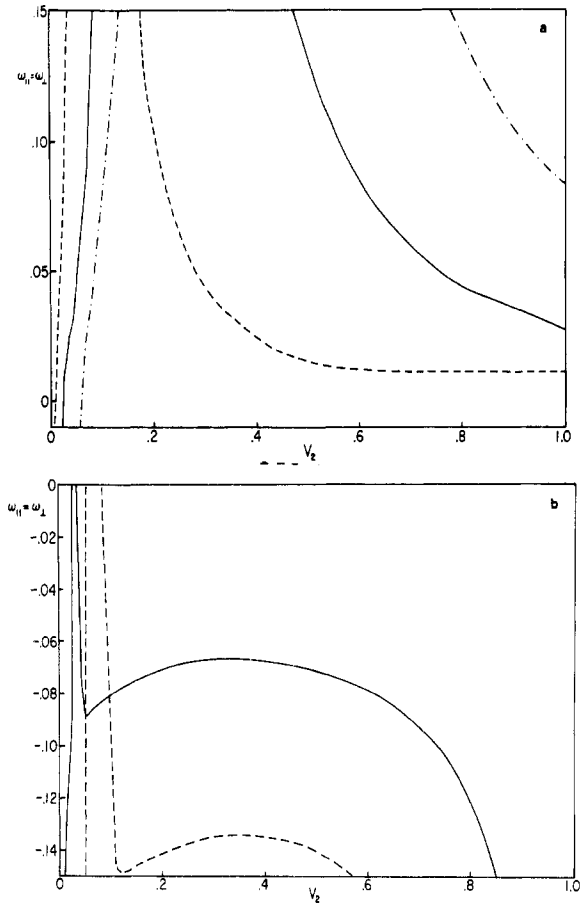

Figure 3. Dependence of the phase behavior on intermolecular interactions, as predicted by the extended DiMarzio model with $\delta = 0.000$, for (a) reversible polymerization with $\phi = -4$ (-·-), $\phi = -5$ (—), and $\phi = -7$ (– – –) and (b) irreversible polymerization with $x = 100$ (—) and $x = 50$ (– – –). In each pair of lines, the left-hand line is the boundary between the two-phase region and the region with a single isotropic phase and the right-hand line is the boundary between the two-phase region and the region with a single anisotropic phase.

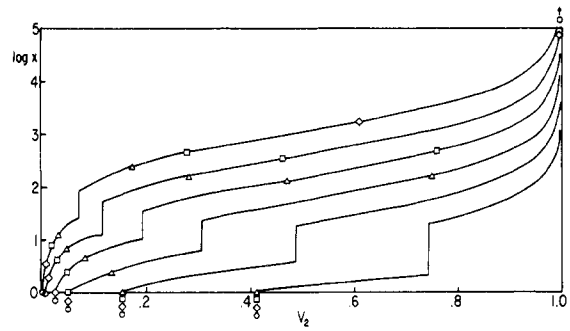

Figure 4. Dependence of rod length in the isotropic and anisotropic conjugate phases on intermolecular interactions: $w_{\parallel} = w_{\perp} = 0.15$ (△), 0.05 (□), 0.01 (◇), 0.00 (○).

unless polymers repel one another, the isotropic phase contains only monomers. In the presence of interpolymer repulsion ($w_{\parallel}$, $w_{\perp} > 0$), polymer length in the isotropic phase increases with increasingly negative free energy of polymerization. Figure 4 also shows that polymer length in the anisotropic phase increases with increasingly negative free energy of polymerization but decreases with increasing repulsion between polymers. The orientation parameter (Figure 2b), on the other hand, is insensitive to these parameters. Repulsive interactions have the effect of pushing the polymers further apart, but this occurs with

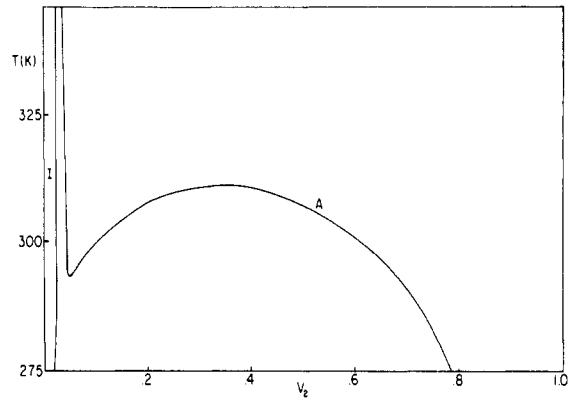

Figure 5. Theoretically predicted temperature dependence of the phase behavior of an irreversibly polymerized system. In this example $x = 100$ and $w_{\parallel} = w_{\perp} = 0.32 - 120/T$. Line I is the boundary between the two-phase region and the region with a single isotropic phase. Line A is the boundary between the two-phase region and the region with a single anisotropic phase.

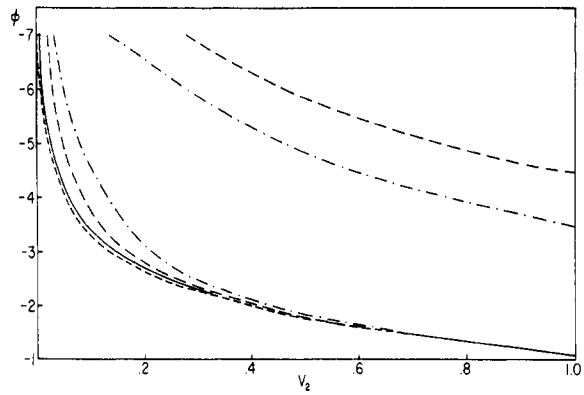

Figure 6. Theoretically predicted dependence of the phase behavior of a reversibly polymerizing system on the free energy of polymerization with $w_{\parallel} = w_{\perp} = -0.15$ (- - -), 0.00 (—), 0.05 (– – –), and 0.15 (-·-). As in Figure 3, the lines mark the boundaries between the region with a single isotropic phase at low v_2, the two-phase region at intermediate v_2, and the region with a single anisotropic phase at high v_2.

negligible loss of order. In this particular, the DiMarzio model generates different results from the Flory model. This may be due to the fact that models which restrict particle orientations to a small discrete set do not sample sharply peaked orientation distributions very well.[21]

Temperature Dependence. For an irreversibly polymerized system, the free energy of interaction between polymers is the only temperature-dependent variable and a T vs. v_2 phase diagram would be expected to be similar in form to those in Figure 3b, provided the forces between polymers are attractive at low temperatures and become less so with increasing temperature. Such an example is given in Figure 5. A phase diagram of this form has been observed for poly(benzyl glutamate) in dimethylformamide.[9,10] For a reversibly polymerizing system, there is a second temperature-dependent variable, the free energy of polymerization. Figure 6 shows more clearly than Figure 3a the calculated dependence of the phase behavior of a reversibly polymerizing system on ϕ. In this representation, and in Figure 3, it is apparent that the boundary between the isotropic region and the two-phase region is relatively insensitive to the interactions between polymers. The position of the boundary between the two-phase region and the anisotropic region is also relatively insensitive to the interactions between polymers above and below the shoulders in Figure 3a. Thus a T vs. v_2 phase diagram for a reversibly polymerizing system will be similar in form

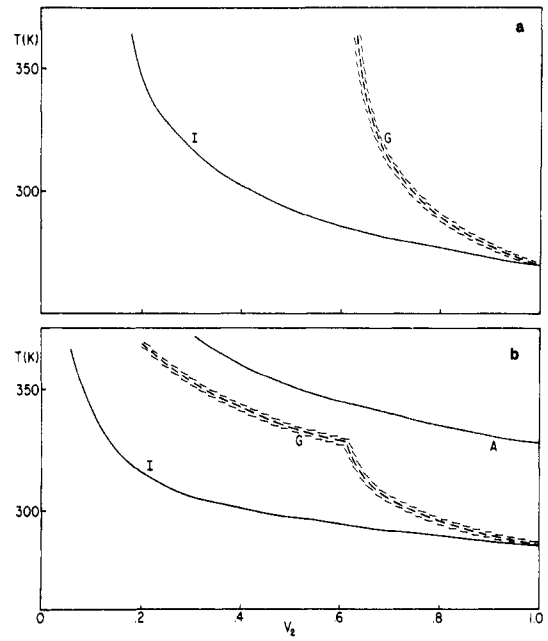

Figure 7. Theoretically predicted temperature dependence of the phase behavior of a reversibly polymerizing system. In these examples, $w_{\parallel} = w_{\perp} = 0.48 - 120/T$ and (a) $\phi = (2400/T) - 10$, (b) $\phi = (6000/T) - 22$. I and A have the same denotation as in Figure 5. The hatched line G is the predicted gelation boundary, assuming that phase separation occurs with spherical domains of colloidal dimensions (see text).

to those in Figure 6, provided that ϕ becomes more negative with increasing temperature (i.e., the enthalpy of polymerization is positive, as in fact is seen in many polymerizing protein systems). Such examples are given in Figure 7.

Comparing Figures 5 and 7, it is apparent that the temperature dependence of the phase behavior of reversibly polymerized molecules is radically different from that of irreversibly polymerized molecules. There exists a temperature T_c, for the reversibly polymerized system, unlike the irreversibly polymerized system, below which there is no phase transition at all. At temperatures just above T_c, the anisotropic phase of the reversibly polymerizing system generally excludes solvent completely ($v_2 \rightarrow 1$). At still higher temperatures the anisotropic phase may be less concentrated if the polymers repel one another and ϕ is sufficiently negative (compare parts a and b of Figures 7).

The phase diagrams in Figure 7 form a basis for predicting the temperature and concentration dependence of the macroscopic properties of reversibly polymerizing systems at equilibrium. The dilute isotropic phase, consisting of monomers or short polymers, should be relatively fluid. The anisotropic phase, consisting of extremely long polymers in highly ordered array, should be relatively rigid. In the two phase region, the rheological properties of the system should depend on the size of the domains formed. If the anistropic domains are small ($\lesssim 10^{-4}$ cm) and dispersed uniformly in the isotropic phase, the system may be regarded as a colloidal suspension of solid particles. The concentration dependence of the viscosity of such a suspension may be described approximately by Brodnyan's[25] extension of Mooney's[26] equation

$$\ln \frac{\eta}{\eta_0} = \frac{2.5 + 0.399(p-1)^{1.48}}{1 - k\Phi}\Phi \qquad (21)$$

where p is the axial ratio of the particles, Φ is the volume fraction of the particles, and k is a crowding parameter with a theoretical maximum value of 1.91. For spheres ($p = 1$), k is approximately equal to 1.56, in the absence of long-range interactions between particles.[27] According to this model, as pointed out previously by Minton,[24] the viscosity of the two-phase region would be expected to rise abruptly as Φ increases beyond ~ 0.4, and "gelation" should occur before Φ reaches 0.5.

Applying this approach to our system, we show with hatched lines in Figure 7 the approximate location of the expected gelation transition, assuming spherical domains ($p = 1, k = 1.56$). Notice that this transition occurs subsequent (higher T or higher v_2) to phase separation, and anisotropic domains may be present before (lower T or lower v_2) gelation. Notice also that there exists a temperature below which the gelation transition is not expected to occur. Such a critical temperature does not exist for irreversibly polymerized systems. (Compare our Figure 7 with Figure 8 of ref 24.) According to eq 21, the actual value of Φ at which gelation would be expected to occur depends on k and p, which both increase with increasing particle asymmetry. Since the domains formed by the alignment of very long polymers are likely to be elongated, rather than spherical, the actual gelation transition should occur to the left of the gelation boundary "G" shown in Figure 7 but would still be located to the right of the phase separation boundary "I" and have the same qualitative "elbow" shape. If the domains are highly elongated, or if the two-phase region is narrow, the gelation transition may nearly coincide with the onset of phase separation. In addition, the formation of highly elongated domains may result in thixotropic behavior. If phase separation occurs with large domains ($\gtrsim 10^{-4}$ cm) a colloidal suspension will not be formed; the anisotropic phase will separate out, leaving behind a fluid isotropic phase, and gelation will not occur.

Sickle-Cell Hemoglobin

The applicability of the foregoing model to the polymerization of sickle-cell hemoglobin and other proteins is limited in a number of respects. To begin with, the model incorporates only the processes of linear polymerization and alignment; higher degrees of ordering and formation of other structures are not considered. Secondly the model is an equilibrium model and applies only to situations at equilibrium with respect to polymerization and alignment. Furthermore, we have assumed that all polymers within a given phase are of the same length (monodispersity). This relatively strong assumption, made for the sake of mathematical tractability, excludes, in particular, the coexistence of monomer and polymer within the same phase. In spite of the above limitations it is useful to examine the extent to which our calculations are consistent with experimental observations of sickle-cell hemoglobin and to consider how this may elucidate the underlying mechanisms.

At sufficiently high temperatures, concentrated solutions of deoxygenated sickle-cell hemoglobin form highly viscous gels. At high concentrations the gels are uniformly birefringent, but at lower concentrations the gels contain spindle-shaped birefringent bodies separated by isotropic material.[28,29] Electron microscopy reveals bundles of parallel filaments.[30-33] Quantitative study of the phase behavior of deoxygenated sickle-cell hemoglobin is complicated by highly concentration-dependent kinetics and hysteresis. Furthermore data obtained at different pHs with different buffering ions and with different methods of hemoglobin preparation are not directly comparable. We must also exclude ultracentrifugation measurements because, due to our assumption of monodispersity, the

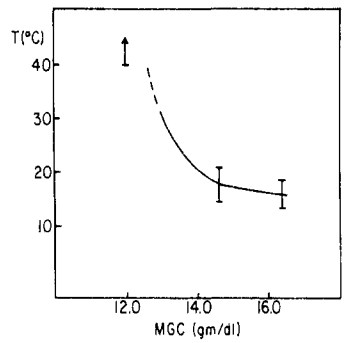

Figure 8. Allison's (1957) measurements of gelation temperatures for sickle-cell hemoglobin solutions of varying concentrations. For a given concentration, the higher temperatures were obtained when increasing T and the lower temperatures when decreasing T.

present model would not be expected to properly describe sedimentation behavior. However, Allison's measurements of the dependence of gelation on concentration and temperature,[29] shown in Figure 8, are qualitatively consistent with the theoretically predicted elbow-shaped curve "G" shown in Figure 7 in that the minimum gelling concentration (MGC) decreases with increasing temperature and that the rate of this decrease itself decreases with increasing temperature. The observation that the minimum gelling concentration is not much greater than the concentration of monomeric hemoglobin in equilibrium with the gel[34-37] suggests, as discussed above, that, under the given experimental conditions, the anisotropic domains are highly elongated or the two-phase region is narrow.

If deoxy sickle-cell hemoglobin solutions are gently stirred while warming, large bundles of aligned fibers are formed and gelation does not occur.[38-41] This is consistent with our expectation that gelation will not occur in the two-phase region if the domain size is sufficiently large. Although large bundles of fibers are also seen in gelled samples, their yield is "much lower" than in stirred samples.[39] The remaining hemoglobin in the gel is presumably organized in smaller bundles to the extent that it is aligned at all. According to the present model, this difference in size and shape distribution between domains in the gelled and stirred systems could be sufficient to explain the differing macroscopic properties of the two systems, without necessarily invoking any differences in the microscopic structure (i.e., alignment and packing of rods) of the anisotropic domains. Under certain conditions of stirring and/or aging, hemoglobin crystals are formed which are structurally and thermodynamically distinct from both the gel and the above quasi-crystalline fiber bundles.[42-45] The present model, however, considers only one-dimensional alignment and does not encompass the possibility of three-dimensional ordering to form crystals.

The time course of sickle-cell hemoglobin gelation has been followed by monitoring heat absorption,[46,47] viscosity,[48-50] birefringence,[46,47,51] scattered light,[52-53] turbidity,[37,51,54] and proton magnetic relaxation.[51,55-58] In each case, there is an initial highly concentration-dependent delay, during which little or no change in the physical property is observed, followed by a rapid change which, except for the birefringence, terminates quickly.

The progress curves have been explained by a model of polymerization involving nucleation and monomer addition.[46,59] In this view, polymer growth is reflected in the curves for heat absorption[47] and proton magnetic relaxation.[60,61] Since the development of birefringence reflects polymer alignment,[62] it is expected to lag behind the calorimetric and magnetic relaxation changes. The turbidity and viscosity changes, on the other hand, are less well understood. Light scattering may be produced both by individual polymers and by domain interfaces. Ferrone et al. have found that the light scattering progress curves conform more closely to theoretical predictions for nucleated polymerization at short times than at long times and suggest that an additional process is operative at longer times.[53] If light scattering at domain interfaces is significant, the long time changes in turbidity may provide a measure of the progress of domain formation. Viscosity progress curves also show an additional process operative at long times. After the initial delay period, a rapid rise in viscosity is followed by a decline.[49,63-65] Since these measurements are made under continuous shear, the hemoglobin polymers would be expected to be aligned as they are formed. Thus the distinct stage of viscosity decline may reflect domain growth which reduces the area of the interface between phases. In general, to the extent that different physical properties vary in their sensitivity to domain formation, comparison of gelation progress curves obtained by different techniques may provide information concerning this process.

Acknowledgment. We are grateful to Allen Minton for sharing with us some of the unpublished details of his calculations for polymers of fixed length. This work was supported by U.S. Public Health Service Grants GM23316, AM21077, and HL07451. J.H. is supported by a Faculty Research Award from the American Cancer Society.

Appendix

The first derivatives of the free energy function, f, given by eq 5, are zero when

$$\ln\left(v_1 + \frac{y}{x}v_2\right) + \frac{2}{y} = 0 \qquad \text{(A1a)}$$

and

$$\ln v_2 - \ln(xy^2) - y\ln\left(v_1 + \frac{y}{x}v_2\right) - \phi = 0 \qquad \text{(A1b)}$$

Combining these equations gives the result that

$$\ln v_2 - \ln(xy^2) + 2 - \phi = 0 \qquad \text{(A1c)}$$

when the first derivatives of f are zero. Combining eq A1a and A1c, we find that the values of x for which the first derivatives of f are zero satisfy the equations

$$x = yv_2/(e^{-2/y} - v_1) \qquad \text{(A2a)}$$

and

$$x = v_2e^{2-\phi}/y^2 \qquad \text{(A2b)}$$

Equating these expressions gives the result that

$$g(y) = y^3e^{\phi-2} - (e^{-2/y} - v_1) = 0 \qquad \text{(A3)}$$

when the first derivatives of f are zero. The function $g(y)$ has a minimum at the value of y for which

$$dg/dy = 3y^2e^{\phi-2} - e^{-2/y}(-2/y^2) = 0 \qquad \text{(A4a)}$$

i.e., at y such that

$$3y^4e^{\phi-2} + 2e^{-2/y} = 0 \qquad \text{(A4b)}$$

and has either no zeroes or a pair of zeroes, one at $3y^4e^{\phi-2} < 2e^{-2/y}$ and one at $3y^4e^{\phi-2} > 2e^{-2/y}$. Since the zeroes occur only for $y \geq 0$, it follows that

$$e^{-2/y} - v_1 < 1 - v_1 < v_2 \qquad \text{(A5a)}$$

and therefore from eq A2a that

$$x = yv_2/(e^{-2/y} - v_1) > y \qquad \text{(A5b)}$$

at these points. Thus the two first derivatives of f are zero at either two points or no points in the region $0 < y < x$.

When the first derivatives of f are zero, the second derivatives, given by eq 6a–c, reduced to

$$\frac{\partial^2 f}{\partial y^2} = \frac{v_2}{x}\left(\frac{2}{y^2} - y^2 e^{\phi-2} e^{2/y}\right) \qquad \text{(A6a)}$$

$$\frac{\partial^2 f}{\partial x \partial y} = \frac{v_2}{x^2}(y^3 e^{\phi-2} e^{2/y}) \qquad \text{(A6b)}$$

$$\frac{\partial^2 f}{\partial x^2} = \frac{v_2}{x^3}(1 - y^4 e^{\phi-2} e^{2/y}) \qquad \text{(A6c)}$$

and

$$\Delta = \frac{{v_2}^2}{x^4}\left(\frac{2}{y^2} - 3y^2 e^{\phi-2} e^{2/y}\right) \qquad \text{(A6d)}$$

For the first zero of $g(y)$, $3y^4 e^{\phi-2} < 2e^{-2/y}$ and therefore $\partial^2 f/\partial x^2 > 0$, $\partial^2 f/\partial y^2 > 0$ and $\Delta > 0$. For the second zero of $g(y)$, $3y^4 e^{\phi-2} > 2e^{-2/y}$ and therefore $\Delta < 0$. Thus the first zero of $g(y)$ corresponds to a local minimum in f and the second corresponds to a saddle point.

References and Notes

(1) Onsager, L. *Ann. N.Y. Acad. Sci.* **1949**, *51*, 627–59.
(2) Isihara, A. *J. Chem. Phys.* **1951**, *19*, 1142–7.
(3) Zwanzig, R. *J. Chem. Phys.* **1963**, *39*, 1714–21.
(4) Flory, P. J. *Proc. R. Soc. London, Ser. A* **1956**, 234, 73–89.
(5) DiMarzio, E. A. *J. Chem. Phys.* **1961**, *35*, 658–69.
(6) Robinson, C. *Trans. Faraday Soc.* **1956**, *52*, 571–92.
(7) Hermans, J. *J. Colloid Sci.* **1962**, *17*, 638–48.
(8) Nakajima, A.; Hayashi, T.; Ohmori, M. *Biopolymers* **1968**, *6*, 973–82.
(9) Wee, E. L.; Miller, W. G. *J. Phys. Chem.* **1971**, *75*, 1446–52.
(10) Miller, W. G.; Wu, C. C.; Wee, E. L.; Santee, G. L.; Rai, J. H.; Goebel, K. G. *Pure Appl. Chem.* **1974**, *37*, 37–58.
(11) Miller, W. G.; Rai, J. H.; Wee, E. L. In "Liquid Crystals and Ordered Fluids"; Johnson, J. F., Porter, R. S., Eds.; Plenum: New York, 1974; Vol. 2, pp 243–55.
(12) Papkov, S. L. *Khim. Volokna* **1973**, *15*, 3.
(13) Papkov, S. P.; Kalichikhin, V. G.; Halmykova, V. D. *J. Polym. Sci., Polym. Phys. Ed.* **1974**, *12*, 1753–70.
(14) Morgan, P. W. *Polym. Prepr., Am. Chem. Soc., Div. Polym. Chem.* **1976**, *17*, 47–52.
(15) Kwolek, S. L.; Morgan, P. W.; Schaefgen, J. R.; Gulrich, L. W. *Polym. Prepr., Am. Chem. Soc., Div. Polym. Chem.* **1976**, *17*, 53–8.
(16) Flory, P. J.; Abe, A. *Macromolecules* **1978**, *11*, 1119–22.
(17) Abe, A.; Flory, P. J. *Macromolecules* **1978**, *11*, 1122–6.
(18) Flory, P. J.; Frost, R. S. *Macromolecules* **1978**, *11*, 1126–33.
(19) Frost, R. S.; Flory, P. J. *Macromolecules* **1978**, *11*, 1134–8.
(20) Briehl, R. W.; Herzfeld, J. *Proc. Natl. Acad. Sci. U.S.A.* **1979**, *76*, 2740–4.
(21) Straley, J. P. *J. Chem. Phys.* **1972**, *57*, 3694–5.
(22) Straley, J. P. *Mol. Cryst. Liq. Cryst.* **1973**, *22*, 333–57.
(23) Flory, P. J.; Ronca, G. *Mol. Cryst. Liq. Cryst.* **1979**, *54*, 289–310.
(24) Minton, A. P. *J. Mol. Biol.* **1974**, *82*, 483–98.
(25) Brodnyan, J. G. *Trans. Soc. Rheol.* **1959**, *3*, 61–8.
(26) Mooney, M. *J. Colloid Sci.* **1951**, *6*, 162–70.
(27) Brodnyan, J. G.; Kelley, E. *J. Colloid Sci.* **1965**, *20*, 7–19.
(28) Harris, J. W. *Proc. Exp. Biol. Med.* **1950**, *75*, 197–201.
(29) Allison, A. C. *Biochem. J.* **1957**, *65*, 212–9.
(30) White, J. G. *Blood* **1968**, *31*, 561–79.
(31) White, J. G.; Heagan, B. *Am. J. Pathol.* **1970**, *58*, 1–17.
(32) Bertles, J. F.; Rabinowitz, R.; Döbler, J. *Science* **1970**, *169*, 375–7.
(33) Finch, J. T.; Perutz, M. F.; Bertles, J. F.; Döbler, J. *Proc. Natl. Acad. Sci. U.S.A.* **1973**, *70*, 718–22.
(34) Bookchin, R. M.; Nagel, R. L. *J. Mol. Biol.* **1973**, *76*, 233–9.
(35) Moffat, K. *Science* **1974**, *185*, 274–7.
(36) Magdoff-Fairchild, B.; Toillon, W. N.; Li, T.-I.; Bertles, J. F. *Proc. Natl. Acad. Sci. U.S.A.* **1976**, *73*, 990–4.
(37) Hofrichter, J.; Ross, P. D.; Eaton, W. A. *Proc. Natl. Acad. Sci. U.S.A.* **1974**, *73*, 3035–9.
(38) Pumphrey, J. G.; Steinhardt, J. *Biochem. Biophys. Res. Commun.* **1976**, *69*, 99–105.
(39) Crepeau, R. H.; Dykes, G.; Edelstein, S. J. *Biochem. Biophys. Res. Commun.* **1977**, *75*, 496–502.
(40) Crepeau, R. H.; Dykes, G.; Garrell, R.; Edelstein, S. J. *Nature (London)* **1978**, *274*, 616–7.
(41) Garrell, R. L.; Crepeau, R. H.; Edelstein, S. J. *Proc. Natl. Acad. Sci. U.S.A.* **1979**, *76*, 1140–4.
(42) Pumphrey, J. G.; Steinhardt, J. *J. Mol. Biol.* **1977**, *112*, 359–75.
(43) Jones, M.; Steinhardt, J. *J. Mol. Biol.* **1979**, *129*, 83–91.
(44) Magdoff-Fairchild, B.; Chiu, C. C. *Proc. Natl. Acad. Sci. U.S.A.* **1979**, *76*, 223–6.
(45) Wilson, S. M.; Makinen, M. W. *Proc. Natl. Acad. Sci. U.S.A.* **1980**, *77*, 944–8.
(46) Hofrichter, J.; Ross, P. D.; Eaton, W. A. *Proc. Natl. Acad. Sci. U.S.A.* **1974**, *71*, 4864–8.
(47) Ross, P. D.; Hofrichter, J.; Eaton, W. A. *J. Mol. Biol.* **1975**, *96*, 239–56.
(48) Malfa, R.; Steinhardt, J. *Biochem. Biophys. Res. Commun.* **1974**, *59*, 887–93.
(49) Harris, J. W.; Bensusan, H. B. *J. Lab. Clin. Med.* **1975**, *86*, 564–75.
(50) Kowalczykowski, S.; Steinhardt, J. *J. Mol. Biol.* **1977**, *115*, 201–13.
(51) Eaton, W. A.; Hofrichter, J.; Ross, P. D.; Tschudin, R. G.; Becker, E. D. *Biochem. Biophys. Res. Commun.* **1976**, *69*, 538–47.
(52) Hofrichter, J.; Gethner, J. S.; Eaton, W. A. *Biophys. J.* **1978**, *24*, 20a.
(53) Ferrone, F. A.; Hofrichter, J.; Eaton, W. A. *Biophys. J.* **1979**, *25*, 254a.
(54) Moffat, K.; Gibson, Q. H. *Biochem. Biophys. Res. Commun.* **1974**, *61*, 237–42.
(55) Waterman, M. R.; Yamaoka, K.; Nelson, E. R.; Cottam, G. L. In "Proceedings of the Symposium on Molecular and Cellular Aspects of Sickle Cell Disease"; Hercules, J. I., Cottam, G. L., Waterman, M. R., Schechter, A. N., Eds.; Department of Health, Education and Welfare: Washington, D.C., 1976; Publication No. (NIH) 76-1007, pp 87–109.
(56) Cottam, G. L.; Waterman, M. R. *Arch. Biochem. Biophys.* **1976**, *177*, 293–8.
(57) Waterman, M. R.; Cottam, G. L. *Biochem. Biophys. Res. Commun.* **1976**, *73*, 639–45.
(58) Shibata, K.; Waterman, M. R.; Cottam, G. L. *J. Biol. Chem.* **1977**, *252*, 7468–74.
(59) Hofrichter, J.; Ross, P. D.; Eaton, W. A. In ref 55, pp 185–222.
(60) Thompson, B. C.; Waterman, M. R.; Cottam, G. L. *Arch. Biochem. Biophys.* **1975**, *166*, 193–200.
(61) Lindstrom, T. R.; Koenig, S. H. *J. Magn. Reson.* **1974**, *15*, 344–53.
(62) Hofrichter, J. *J. Mol. Biol.* **1975**, *96*, 254–6.
(63) Goldberg, M.; Bunn, H. F.; Muss, H.; Harkness, D. In ref 55, pp 133–41.
(64) Briehl, R. W. *Fed. Proc., Fed. Am. Soc. Exp. Biol.* **1979**, *38*, 460.
(65) Briehl, R. W. In "Symposium on the Molecular Basis of Mutant Hemoglobin Disfunction, University of Chicago, October 1979"; Sigler, P. B., Ed., in press.